SKI Report 01:2

Research

Susceptibility of Copper to General and Pitting Corrosion in Highly Saline Groundwater

Timo Laitinen
Kari Mäkelä
Timo Saario
Martin Bojinov

January 2001

ISSN 1104-1374
ISRN SKI-R–01/2–SE

SKI Report 01:2

Research

Susceptibility of Copper to General and Pitting Corrosion in Highly Saline Groundwater

Timo Laitinen
Kari Mäkelä
Timo Saario
Martin Bojinov

VTT Manufacturing Technology, Materials and Structural Integrity,
P.O. Box 1704, FIN-02044 Espoo, Finland

January 2001

SKI Project Number 99200

CONTENTS

PREFACE

This work has been performed as part of the research program funded by the Swedish Nuclear Power Inspectorate (SKI) and Finnish Radiation and Nuclear Safety Authority (STUK) and aimed at verification of the safety of nuclear fuel waste disposal concept. The research program consists of a series of research projects. The reports from this research program published earlier are

(1) STUK-YTO-TR 105 (1996), "Environmentally assisted cracking behaviour of copper in simulated ground water,

(2) STUK-YTO-TR 106 (1996), "Electrical properties of oxide films formed on copper in 0.1 M borax solution",

(3) SKI Report 96:80 (1996), "The effect of nitrite ion on the electric properties of oxide films on copper",

(4) STUK-YTO-TR 134 (1997), "The effect of chlorides on the electric properties of oxide films on copper",

(5) SKI Report 99:27 (1999), "Surface films and corrosion of copper" and

(6) STUK-YTO-TR 157 (1999), "Electric and electrochemical properties of surface films formed on copper in the presence of bicarbonate ions".

The project reported here has been funded by SKI. Co-operation with Christina Lilja, SKI, is gratefully acknowledged.

Espoo, December 30, 2000

Authors

1 SUMMARY

In Sweden and Finland the spent nuclear fuel is planned to be encapsulated in cast iron canisters that have an outer shield made of copper, which is responsible for the corrosion protection. In this work the susceptibility of Cu OFP to general and pitting corrosion was investigated in highly saline groundwater at T = 80 °C and p = 14 MPa using electrochemical techniques in autoclave conditions. The effect of pressure was investigated by conducting tests at p = 2, 7 and 14 MPa. The main observations made are:

- Because pressure has a clear effect on the voltammetric and electrochemical impedance spectroscopy response of Cu OFP, this kind of tests should be performed at the representative pressure of 14 MPa.
- The corrosion potential of Cu OFP in all test runs was in the range of -0.15 V_{SHE} < E_{corr} < -0.08 V_{SHE}.
- At the corrosion potential active dissolution (corrosion) of Cu OFP takes place. The corrosion rate based on weight loss measurements of corrosion coupons after a seven day exposure was 0.02 mm/y.
- The measurement results are in line with the thermodynamic calculations presented in the SKI Report 98:19, concerning the influence of Cl^- content on the dissolution of copper.

SAMMANFATTNING

Slutförvaringen av använt kärnbränsle har i Sverige och Finland tänkt skötas genom inkapsling av bränslet i gjutjärnskapslar med ett kopparhölje som skyddar mot korrosion. I denna rapport behandlas koppars (Cu-OFP) sensitivitet (känslighet) för allmän och lokal korrosion (gropfrätning) i grundvatten med hög salthalt under förhöjd temperatur (T=80°C) och tryck (p=14 MPa). De rätta omgivningsförhållandena åstadkomms med VTT:s autoklavutrustning och de utförda mätningarna och resultaten baserar sig på elektrokemiska metoder utvecklade och anpassade för denna sorts försök. Tryckets betydelse undersöktes genom försök på tre trycknivåer, nämligen 2, 7 och 14 MPa. De viktigaste observationerna från dessa försök är:

- Eftersom tryck har en direkt verkan på voltametrisk och elektrokemisk impedans spectroskopi hos Cu-OFP bör mätningarna genomföras under representativt tryck (14 MPa)
- Korrosionspotentialen (E_{Corr}) hos Cu-OFP var för alla försök inom spänningsintervallet -0.08 till -0,15 V_{SHE}. Korrosion och upplösning av Cu-OFP sker då korrosionspotentialen uppnåtts.
- Korrosionshastigheten uppmättes till 0.02 mm/y genom mätning av den viktförlust som uppstod vid sju dygns exponering.
- Mätresultaten är jämförbara med de termodynamiska beräkningarna rapporterade i SKI:s rapport 98:19, gällande klorets (Cl^-) inverkan på koppars upplösning.

2 INTRODUCTION

In Sweden and Finland the spent nuclear fuel is planned to be encapsulated in cast iron canisters that have an outer shield made of copper. The copper shield is responsible for the corrosion protection of the canister construction.

The pressure in the final disposal vault is built up by two components. The first part consists of the hydrostatic pressure of water. This part depends on the depth at which the vault is built. If the vault is at the depth of 700 m, the hydrostatic pressure increases up to 7 MPa. The bentonite clay surrounding the copper canister will swell when it is wetted. This causes an additional pressure, which is estimated to be 7 MPa. Thus the total pressure estimated to prevail in the vault at the copper canister surface is then a maximum of 14 MPa.

The first goal of this work was to determine the effect of pressure on electrochemical behaviour of Cu OFP in groundwater conditions (T = 80 °C, p = 2, 7 and 14 MPa), representative of those predicted for the final disposal vault. The second goal was to study general and pitting corrosion susceptibility as well as the properties of surface films possibly forming on Cu OFP in the same groundwater conditions (T = 80 °C, p = 14 MPa). The simulated groundwater used in this work is highly saline thus representing a composition one does not expect to find under ordinary conditions. However, in some borehole investigations similar salinity levels have been found at repository depth. These have been interpreted to be remnants of ancient seawater buried in the bedrock.

3 EXPERIMENTAL

Phosphorus microalloyed copper (Cu OFP, containing 99.992 wt-% Cu and 45 ppm P, Outokumpu Poricopper Oy) was used as the test material in all the experiments. The working electrodes were polished using 4000 grit emery paper and rinsed with MILLI-Q® water before use. The experiments were performed in a static AISI 316 stainless steel autoclave. The electrolyte was deaerated and pressurised to the test pressure using nitrogen gas. During the experiments, nitrogen gas was continuously bubbled through the electrolyte in the autoclave. An external pressure balanced AgCl/Ag reference electrode filled with 0.1 M KCl was installed into the autoclave. Additionally, a Pd electrode saturated with hydrogen was used as a reference and was assumed to behave as a Reversible Hydrogen Electrode (RHE). All the potentials in this work are reported on the standard hydrogen electrode scale. The groundwater composition is given in Table 1. This composition is representative of the highly saline groundwater, and is called brine near-field reference water /1/. The solutions were made of p.a. NaCl, p.a. Na_2SO_4, p.a. $MgSO_4$, p.a. $CaCl_2$, p.a. KCl, p.a. $NaHCO_3$ and MILLI-Q® purified water. The pH of the solution was 7.6 after preparation and 6.6 after storing in a glass vessel for six months.

Table 1. *Composition of the groundwater (mg/l).*

Cl^-	SO_4^{2-}	Mg^{2+}	Ca^{2+}	Na^{2+}	K^+	HCO_3^-
53800	1200	700	9900	22700	190	4.8

The potential difference between the Pd electrode and the AgCl/Ag reference electrode filled with 0.1 M KCl can be used as a measure of the pH. The calculated difference between the potential of the AgCl/Ag reference electrode filled with 0.1 M KCl and the standard hydrogen electrode scale (SHE) is 0.231 V at T = 80 °C ($E^0_{H^+/H_2} = E_{SHE} = E_{AgCl/Ag} - 0.231V$). The Nernst equation relates the pH_T and potential E_{H^+/H_2} at 80 °C as follows

$$E_{H^+/H_2} = E^0_{H^+/H_2} + \frac{R \cdot T}{z \cdot F} \cdot \ln \frac{a_{H^+}}{\sqrt{f_{H_2}/0.1MPa}} \qquad (1)$$
$$= E^0_{H^+/H_2} - 0.07V \cdot pH_T - 0.035V \cdot \log(f_{H_2}/0.1MPa)$$

Here f_{H2} is the fugacity (≈ partial pressure) of hydrogen gas in the water. From equation (1) pH_T becomes

$$pH_T = \frac{E_{AgCl/Ag} - E_{H^+/H_2} - 0.231V - 0.035V \cdot \log(f_{H_2}/0.1MPa)}{0.07V} \qquad (2)$$

The potential difference $\Delta E = E_{AgCl/Ag} - E_{H^+/H_2}$ was measured to lie between 0.72 V <ΔE< 0.81 V in the different test runs. The magnitude of hydrogen partial pressure at

the Pd electrode surface is not known precisely. Taking that the hydrogen partial pressure at the Pd electrode surface can be 14 MPa at maximum (equal to the test pressure) one can estimate that the effect of hydrogen partial pressure can be 1.1 pH units at maximum. From these values the estimated $pH_{T=80C}$ is $6.0 < pH_{T=80C} < 8.3$. Assuming a smaller hydrogen partial pressure of 1 MPa and taking the average value of $\Delta E = 0.77$ results in the estimate of $pH_{T=80C} = 7.2$. Comparing this estimate with the value of 7.6 measured at room temperature after preparation indicates that the pH of the solution possibly decreases slightly when heated to 80 °C.

Electrochemical impedance measurements were performed by a Solartron ECI 1287/FRA 1260 system controlled by ZPlot / CorrWare software (Scribner) in a frequency range 0.03 Hz - 10 kHz at an AC amplitude of 10 mV (rms). Voltammetric measurements were performed with the same system. The contact electric resistance (CER) equipment was supplied by Cormet Ltd. Potentiostatic and potentiodynamic conditions during CER measurements were ensured using a Wenking LB 81M potentiostat and a Hi-Tek Instruments PPR1 waveform generator.

4 RESULTS AND DISCUSSION

4.1 Corrosion coupon tests

Three weight loss coupons were exposed to the environment. The coupons were weighed before and after the exposure. The exposure time was seven days. After the exposure the specimen surfaces were examined with the scanning electron microscopy (SEM) for possible pitting corrosion. The surface appearance of the corrosion coupons is shown in Figs 1a to 1d. The appearance is typical for general corrosion. There was no sign of localised corrosion (pitting).

The weight loss measurement results are shown in Table 2.

Table 2. *Corrosion coupon test results.*

Specimen number	1	2	3
Surface area, cm^2	15.84	16.56	14.51
Weight before exposure, g	8.5451	8.9616	10.0933
Weight after exposure, g	8.5417	8.9570	10.0866
Weight loss, g	0.0034	0.0046	0.0067
Corrosion rate, mm/y	0.013	0.016	0.027

The general corrosion rate was calculated using the formula

$$\Delta = \frac{\Delta m \cdot 3650}{\rho \cdot A \cdot t}[mm/y] \qquad (3)$$

where Δm = weight loss [g], ρ = density [g/cm^3], A = surface area [cm^2] and t = exposure time [days]. The density of copper is 8.94 g/cm^3.

The calculated corrosion rates are in the average 0.0185 mm/y. Using a corrosion allowance of 30 mm this would indicate a lifetime of about 1600 years, assuming that the transport of corrosion products away from the surface and that of the reactants towards the surface would be similar to the present experimental situation. However, it is very likely that the rate of transport in bentonite clay is limited, and will therefore possibly become rate limiting and thus slow down the corrosion process.

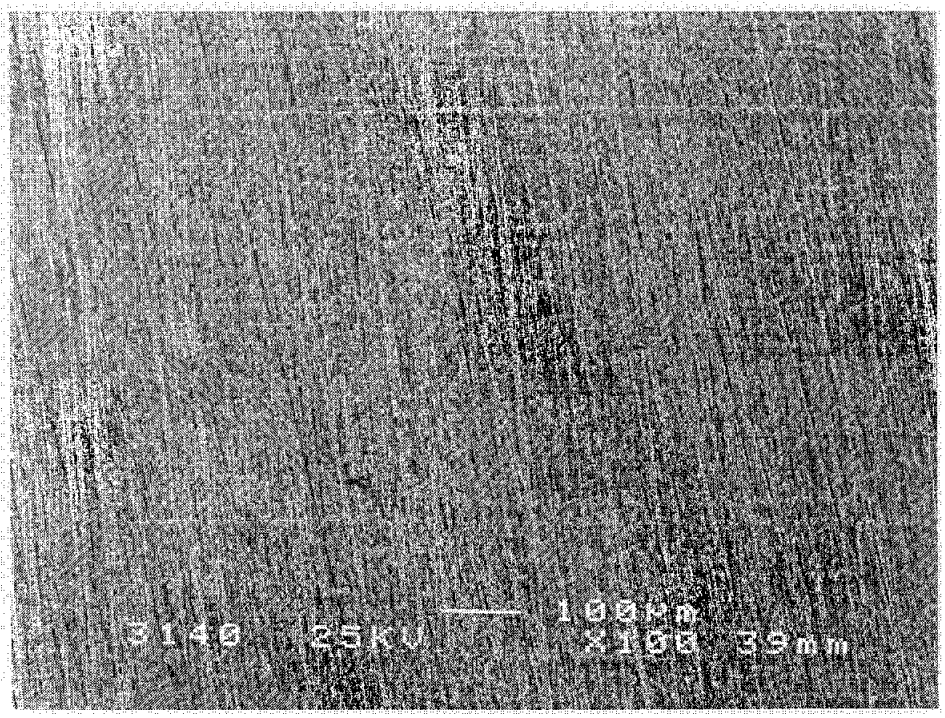

(a) Magnification x 100.

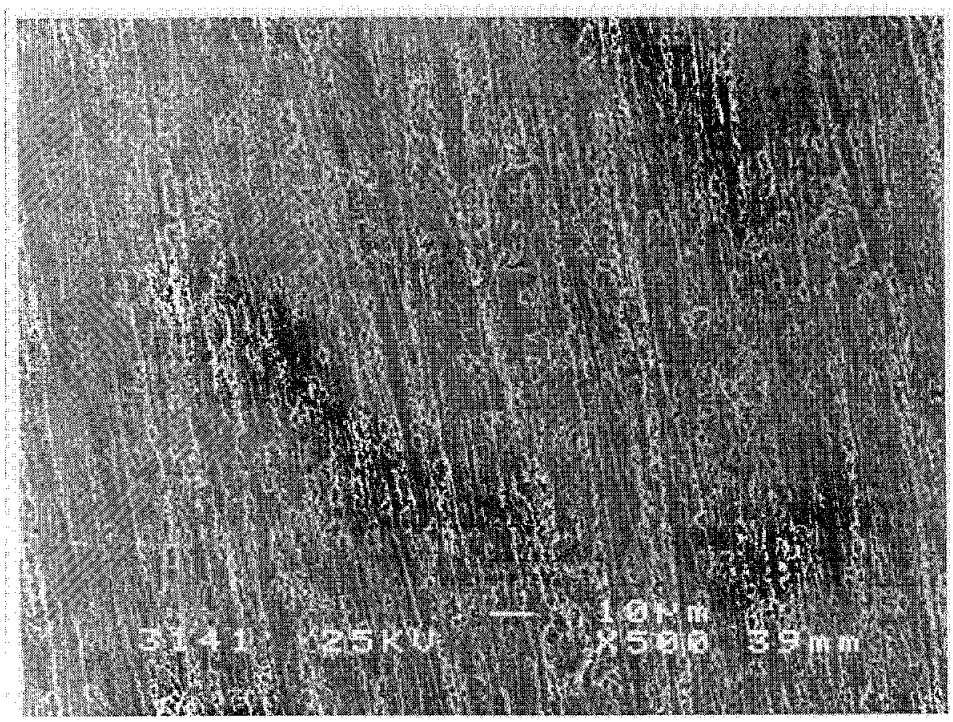

(b) Magnification x 500.

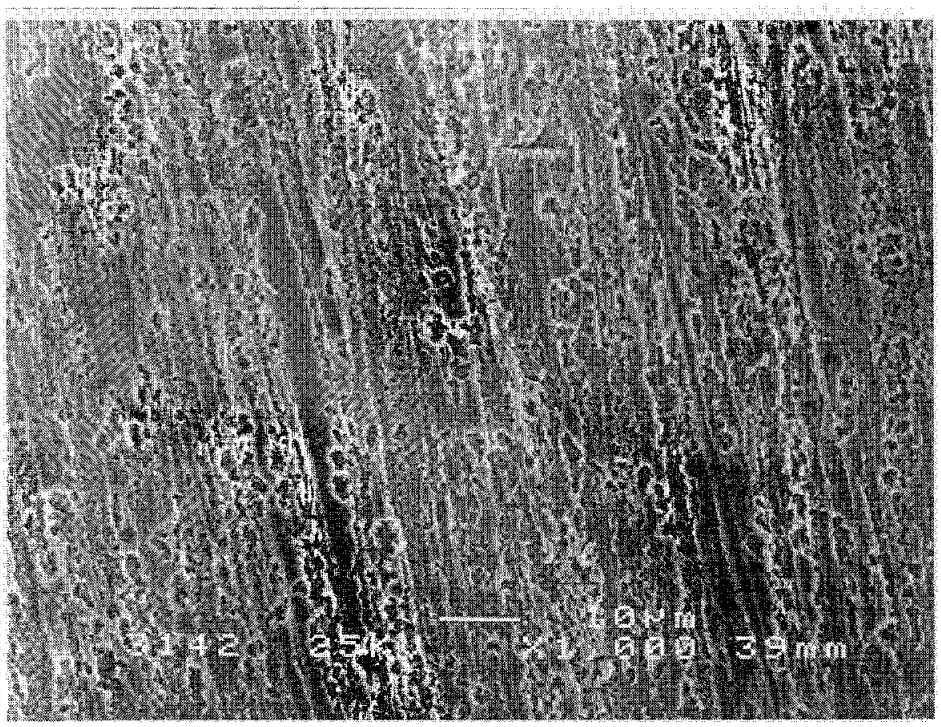

(c) Magnification x 1000.

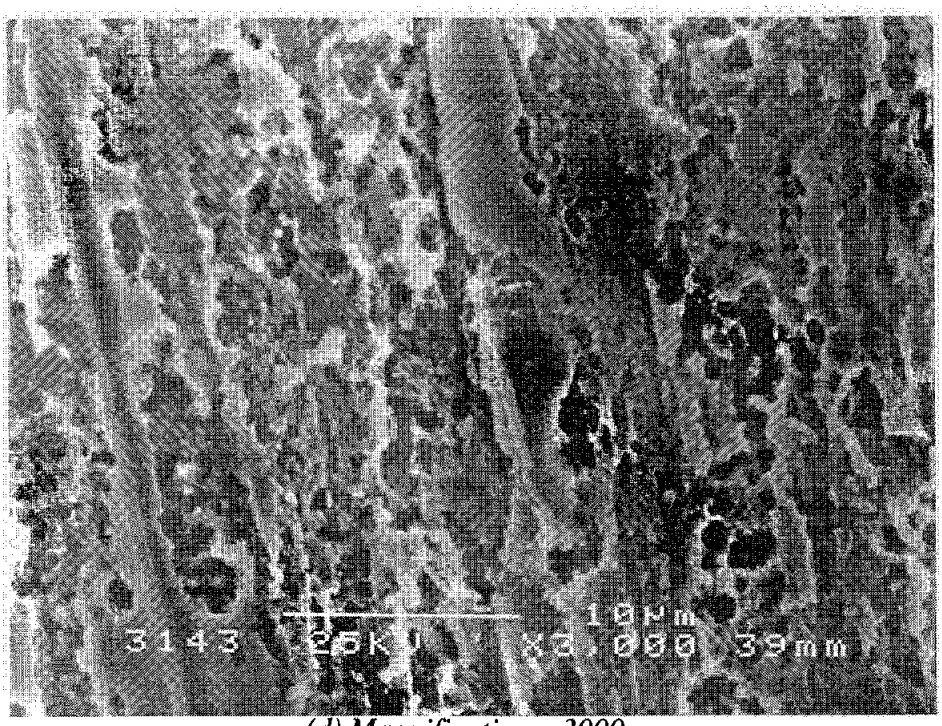

(d) Magnification x 3000.

Figure 1. Scanning electron microscopy images of the surface of Specimen No 3 after the seven day exposure to the highly saline groundwater (80 °C, 14 MPa).

4.2 Voltammetry

The polarisation curve of Cu OFP in the test solution is shown in Fig. 2 at three successively increasing pressures, namely 2, 7 and 14 MPa. The H^+/H_2-equilibrium potential is at -0.47 V. The main features in the three curves are the same; a small increase of current at -0.25 V, a further steep increase of current starting at about -0.05 V and a small reduction peak during the negative-going sweep at about -0.4 V. In the curve measured at the pressure of 14 MPa, the negative current at the starting potential of -0.49 V is about two times higher than at lower pressures, the first increase in positive current is much more pronounced and the peak in the negative-going sweep at around -0.4 V is also better evidenced. The measurement result at three successively decreasing pressures is shown in Fig. 3, indicating that the effect of pressure on the polarisation curves is reversible.

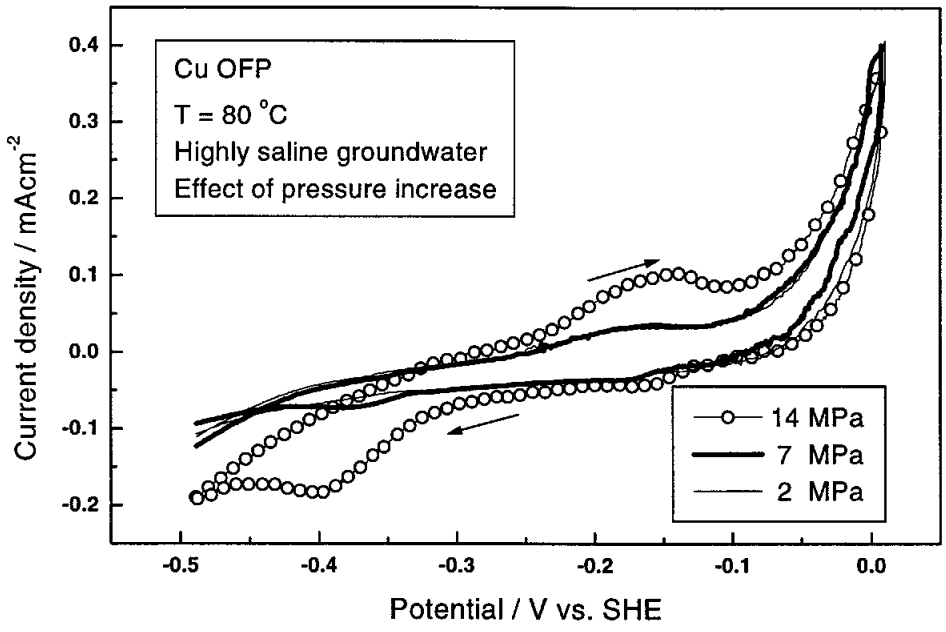

Figure 2. Polarisation curve of Cu OFP in highly saline groundwater at three increasing pressure levels (N_2 gas, continuous bubbling through the autoclave); 2 MPa, 7 MPa and 14 MPa. T = 80 °C, sweep rate 2 mV/s. Not corrected for i-R-drop.

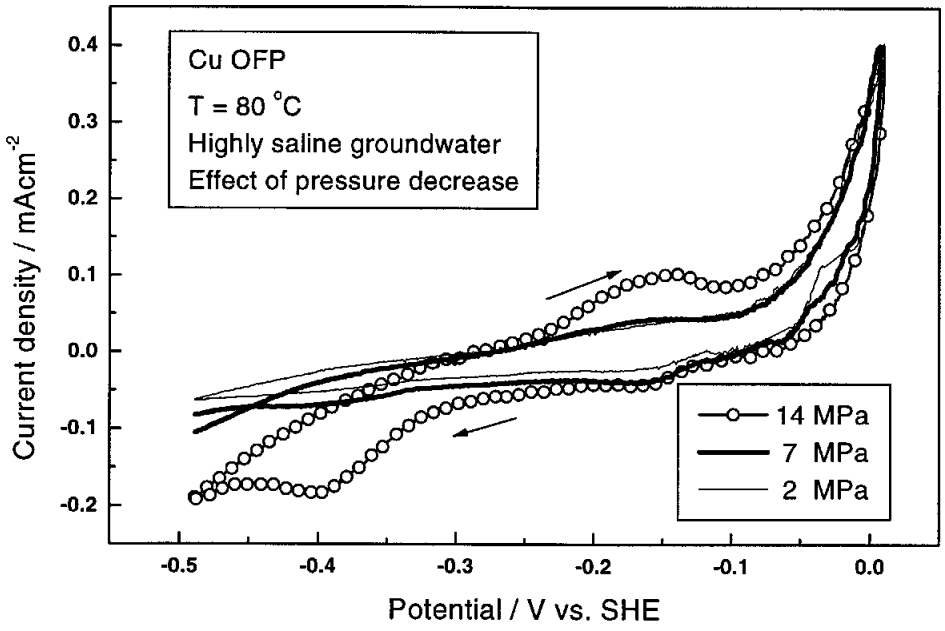

Figure 3. Polarisation curve of Cu OFP in highly saline groundwater at three decreasing pressure levels (N_2 gas, continuous bubbling through the autoclave); 14 MPa, 7 MPa and 2 MPa. T = 80 °C, sweep rate 2 mV/s. Not corrected for i-R-drop.

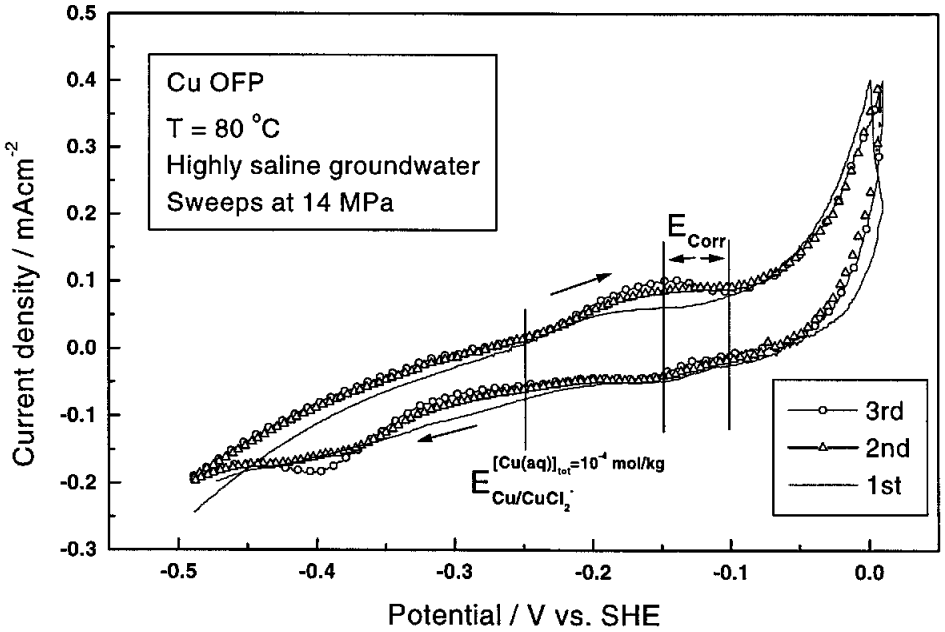

Figure 4. Three consecutive polarisation curves of Cu OFP in highly saline groundwater at the pressure of 14 MPa (N_2 gas, continuous bubbling through the autoclave). T = 80 °C, sweep rate 2 mV/s. Not corrected for i-R-drop.

Three consecutive sweeps were measured at the pressure of 14 MPa, Fig. 4. In the figure, the range of corrosion potentials measured is also indicated, as well as the $CuCl_2^-$/Cu equilibrium potential (as calculated by Beverskog and Puigdomenech /2/ for a concentration $[Cu(aq)]_{tot} = 10^{-4}$ mol/kg). The corrosion potential is roughly 0.1 V higher than the $CuCl_2^-$/Cu equilibrium potential. This reflects the fact that the corrosion potential is a mixed potential determined both by the anodic and cathodic reactions, i.e. oxidation of Cu to $CuCl_2^-$ and reduction of O_2.

Figure 5 shows the polarisation curve of Cu OFP measured in the potential range -0.49 V < E < 0.46 V. A higher sweep rate was used to preserve the specimen as the current density at high positive potentials was found to be very high. The positive current increase starting at about -0.05 V reaches a level which is higher than 40 $mAcm^{-2}$ at E = 0.23 V, after which the current decreases rapidly as potential increases to 0.3 V. At still higher potentials the current increases again. In the negative going sweep a broad reduction peak is seen at -0.2 V < E < 0.05 V. According to the calculations of Beverskog and Puigdomenech /2/, a solid compound of $CuCl_2 \bullet 3Cu(OH)_2$ may be formed on copper in this environment at about +0.4 V. One may thus assume that the decrease in the current seen at about +0.3 V is connected with a formation of a surface film of a composition close to this. It seems, though, that the film is not a real passive film in the sense that a high current still passes through it. The broad reduction peak at -0.2 V < E < 0.05 V is assumed to be connected with reduction of the non-passivating film formed at E > 0.3 V.

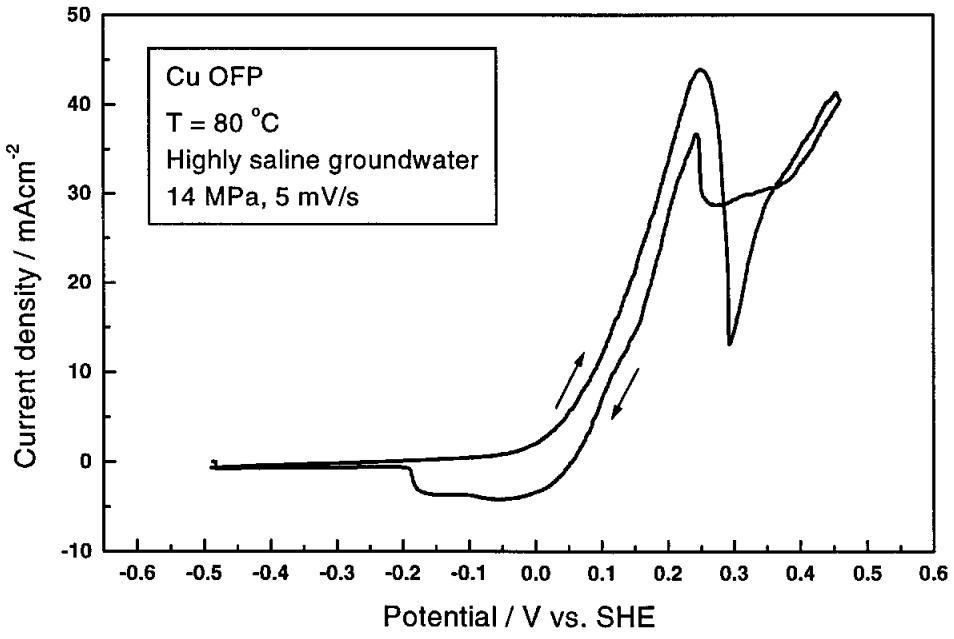

Figure 5. Polarisation curve of Cu OFP in highly saline groundwater at 14 MPa (N_2 gas, continuous bubbling through the autoclave). T = 80 °C, sweep rate 5 mV/s. Not corrected for i-R-drop.

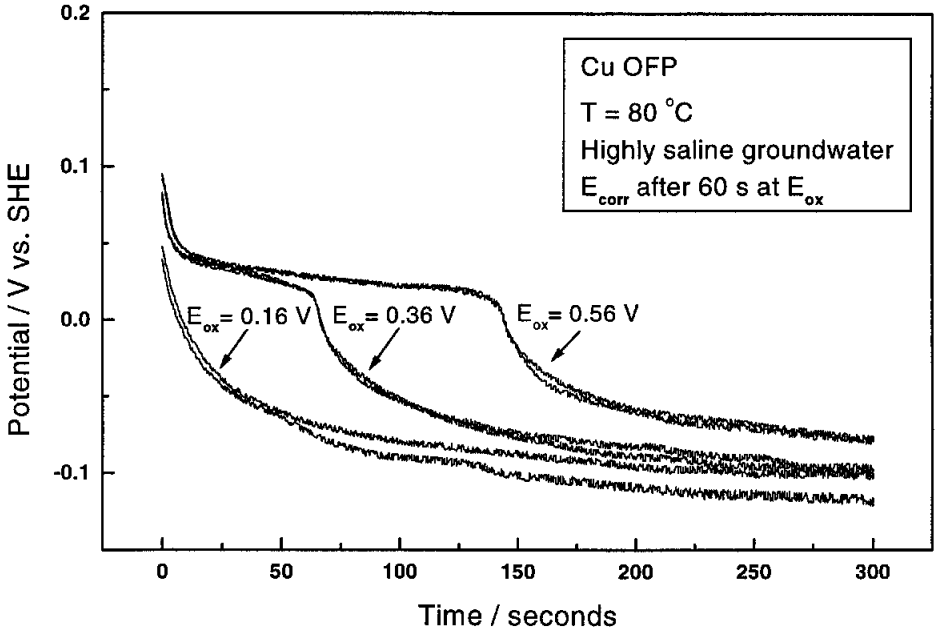

Figure 6. Open circuit potential decay after keeping the specimen at different elevated positive potentials.

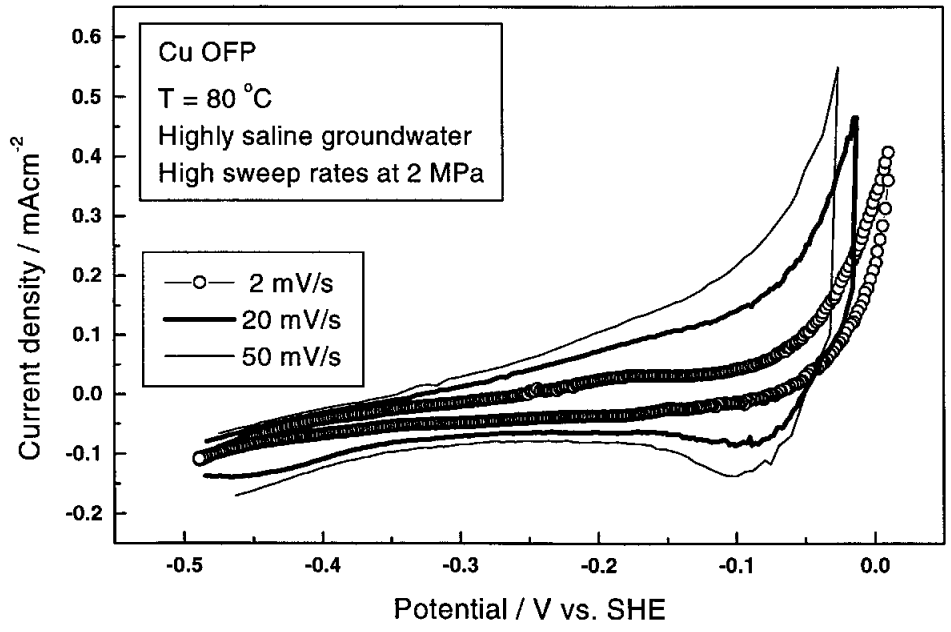

Figure 7. Comparison of polarisation curves measured with different sweep rates.

Figure 6 shows the open circuit potential decay curves after oxidation at three potentials. When the potentiostat is switched off the open circuit potential decreases rapidly (partly due to iR-drop). Comparing with Fig. 5 it is evident that at the potential 0.16 V no film should be formed, whereas both potentials 0.36 V and 0.56 V are in the range where some surface film is formed. In Fig. 6, for the two higher potentials, 0.36 V and 0.56 V, there is a plateau in the open circuit potential. This indicates that at these potentials a surface film is formed, which then reduces during the plateau time. Thus these results are in line with the data shown in Fig. 5.

The effect of increasing sweep rate shown in Fig. 7 is to introduce an increasing reduction peak in the negative going sweep. This may be due to the reduction of $CuCl_2^-$ (or CuCl(aq)) which forms from Cu(I) dissolving during the positive going sweep. In the faster going sweeps $CuCl_2^-$ (CuCl(aq)) has not enough time to diffuse away from the surface and is therefore reduced back to metallic copper and chloride ions.

4.3. Electric resistance of surface

The electric resistance was monitored together with the open circuit potential for a period of about 20 hrs. The very low electric resistance shown in Fig. 8 indicates that the surface has no passive film on it. Such a low electric resistance indicates a metallic surface with possibly some adsorbed anions. The open circuit potential in this exposure was $-0.24\ V < E_{ocp} < -0.18\ V$.

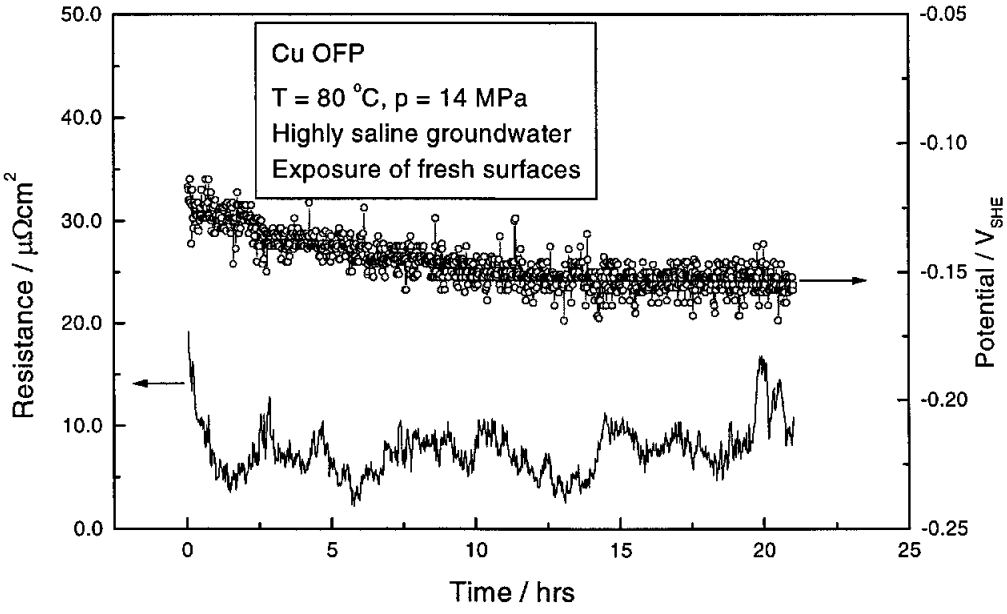

Figure 8. Electric resistance of Cu OFP fresh surfaces exposed to the highly saline groundwater at open circuit potential (E_{corr}).

In a test where the specimen was first polarised to a potential of +0.25 V_{SHE} for 30 seconds and then the polarisation was stopped and the specimen was left at open circuit potential, the resistance decreased with the potential as shown in Fig. 9. This indicates that even though some surface film was formed at +0.25 V_{SHE} it was reduced within about two minutes. However, in another set of similar tests the formation of an unstable surface film at higher potentials was not found to occur. This may indicate that the film formation is sensitive to small variations in the test environment and surface pre-treatment.

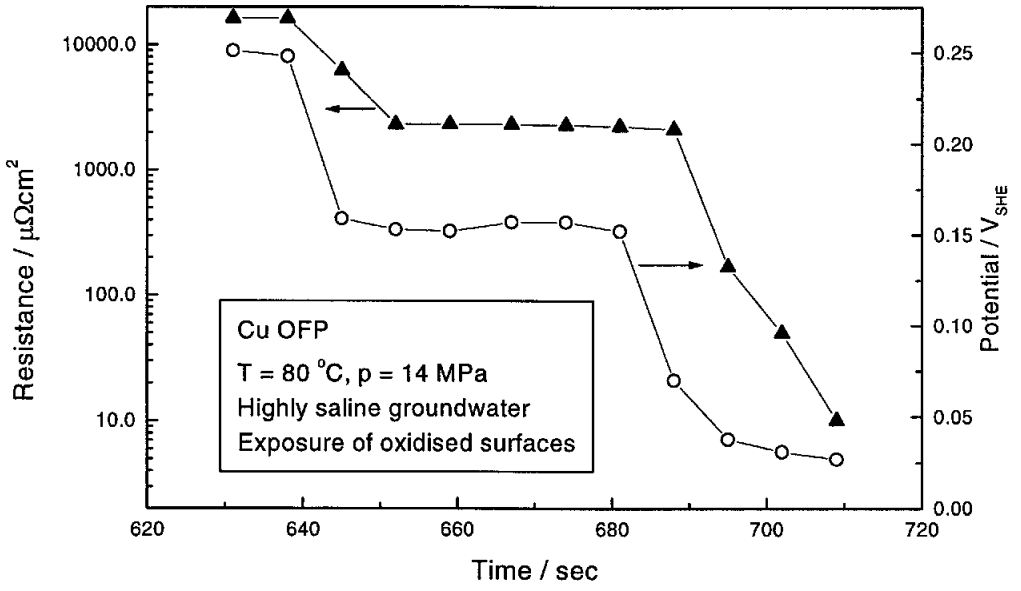

Figure 9. Electric resistance of Cu OFP exposed to the highly saline groundwater at open circuit potential (E_{corr}) after oxidising for 30 seconds at +0.25 V_{SHE}.

4.4 Impedance response of copper

The impedance spectrum of Cu OFP in the test solution was measured several times at the corrosion potential. Figure 10 shows the effect of pressure increase. The stabilisation time at the pressure before the measurement was more than two hours at each pressure level. The results measured at 14 MPa and 7 MPa are rather close to each other, while the result from the measurement at 2 MPa is clearly different, although the main features are the same in all the measurements.

The magnitude of impedance at the highest frequencies is a measure of the electrolyte resistance. A particular feature in these results is that the electrolyte resistance is lower by a factor of about 5 at 14 MPa and 7 MPa in comparison with 2 MPa. This result was well repeatable. At this stage we cannot give a reasonable explanation to this phenomenon.

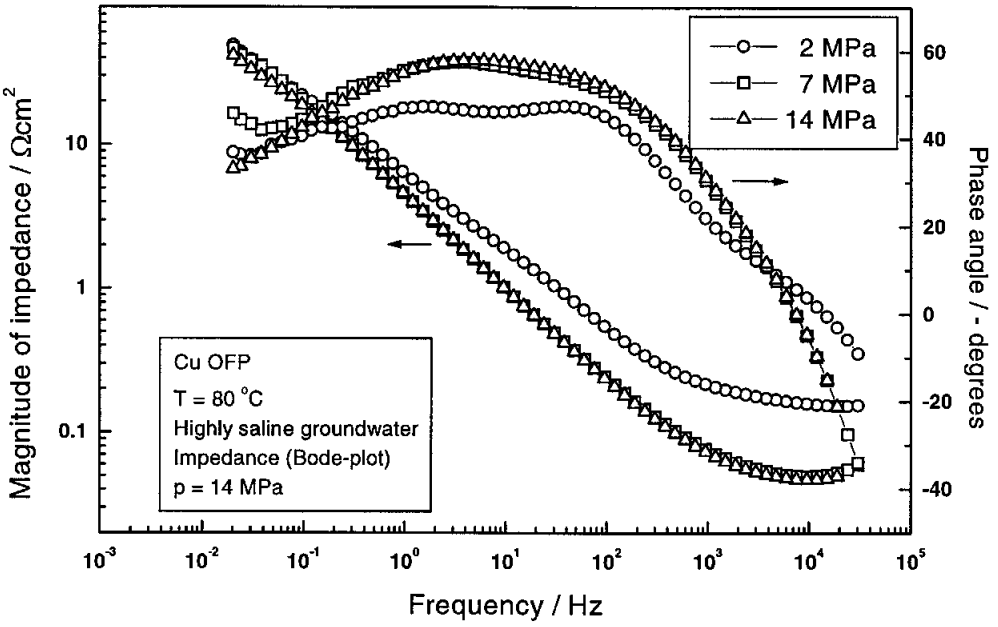

Figure 10. Impedance spectra (Bode-plot) of Cu OFP in the test solution measured at the corrosion potential in highly saline groundwater at three increasing pressure levels (N_2 gas, continuous bubbling through the autoclave); 2 MPa, 7 MPa and 14 MPa. Stabilisation time about two hours.

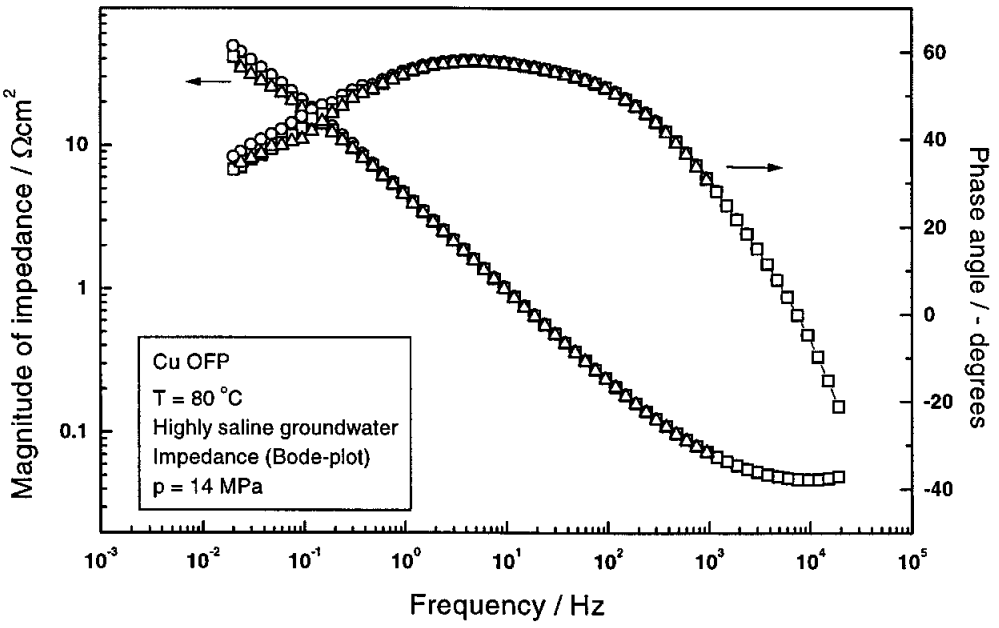

Figure 11. Three consecutive impedance spectra of Cu OFP in the test solution measured at the corrosion potential in highly saline groundwater (p = 14 MPa, N_2 gas, continuous bubbling through the autoclave). Stabilisation time about two hours.

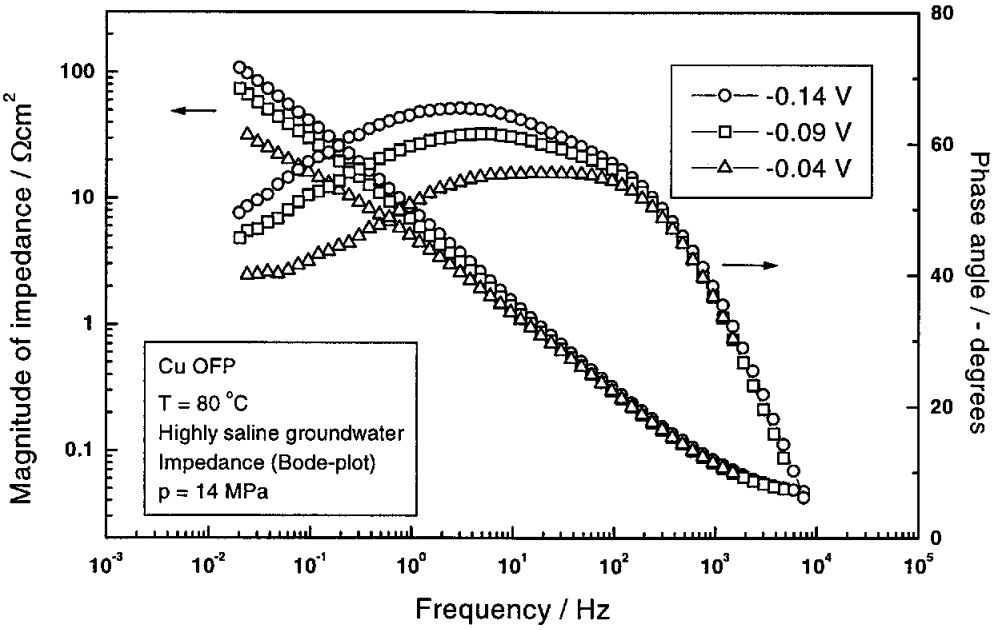

Figure 12. Effect of increasing potential on the impedance spectra (p = 14 MPa, N_2 gas, continuous bubbling through the autoclave). Stabilisation time was about 30 min at each potential.

Results of repeated impedance measurements at the pressure of 14 MPa are shown in Fig. 11. The results were highly repeatable, and indicate a rather low magnitude of impedance of about 100 Ωcm^2 at the limit when f→0 Hz. A passive film with good corrosion resistance, like that forming on Cr and Fe-Cr alloys in aqueous solutions has typically a magnitude of impedance in the range 10^4 $\Omega cm^2 < |Z| < 10^6$ Ωcm^2 /3,4/.

The effect of polarisation to potentials more positive than the open circuit potential is shown in Fig. 12. The magnitude of the impedance at all frequencies decreases as the potential increases. This indicates that the process dominating the spectra is an electrochemical one. The forward part (i.e. oxidation) of an electrochemical reaction is facilitated when the specimen is polarised to more positive potentials because increasing the potential is then equal to increasing the driving force for this reaction. If the reaction in question would be a chemical one then potential should have now influence on the reaction.

The voltammetric and contact electric resistance (CER) results shown above indicate that there is no stable surface film on copper in this environment. The CER results showed very low resistance and the voltammetry results showed that the open circuit potential was in the potential area where no passivation can occur. Thus it is reasonable to assume that copper dissolution takes place at open circuit potential. Dissolution of

copper may occur via different routes. One possibility /5/ is that copper first oxidises to CuCl and adsorbs on the surface, after which it combines with chloride to $CuCl_2^-$ and diffuses further away into the solution. The reactions are as follows:

$$Cu + Cl^- \rightarrow CuCl_{ads} + e^- \qquad \text{electrochemical reaction} \qquad (4a)$$

$$CuCl_{ads} + Cl^- \rightarrow CuCl_2^- \qquad \text{chemical reaction} \qquad (4b)$$

In this process the first step is electrochemical and the second chemical. Another possibility is that copper may dissolve /5/ via the following reactions:

$$Cu \rightarrow Cu^+ + e^- \qquad \text{electrochemical reaction} \qquad (5a)$$

$$Cu^+ + 2Cl^- \rightarrow CuCl_2^- + e^- \qquad \text{chemical reaction} \qquad (5b)$$

Gabrielli et al. /6/ have proposed, based on recent experimental evidence that the process of copper dissolution in neutral solutions is as follows:

$$Cu + Cl^- \rightarrow CuCl_{ads}^- \qquad \text{chemical reaction} \qquad (6a)$$

$$CuCl_{ads}^- \rightarrow CuCl(aq) + e^- \qquad \text{electrochemical reaction} \qquad (6b)$$

The same equivalent circuit can describe the reaction schemes 4a/4b and 6a/6b. The difference is that in the reaction scheme 4a/4b the first reaction, being an electrochemical one, should depend on potential and the resistance associated with it should decrease as potential increases. The resistance of a chemical reaction should not depend on potential. When fitting the data it was found that the resistance associated with the second reaction step decreased markedly while the resistance associated with the first reaction step remained almost constant as a function of potential. Thus the last process sequence proposed by Gabrielli at al. /6/ gave the best fit to the measured impedance data and is considered to be the correct one in our case. King and Kolar in their review /7/ and King and Tang /8/ indicate that their data (Cl^- < 1 M) is best fitted by the above reaction scheme 4a/4b. We found that the model for the reaction scheme 5a/5b, which contains a Gerischer-element to account for diffusion of the Cu^+ away from the surface and the following chemical reaction with Cl^- in the solution could not be fitted well to the data. A Gerischer-element is the electrical equivalent of a process in which a reaction product diffuses away from the surface at which it was formed and then takes part in a chemical reaction further away in the solution.

The equivalent circuit is shown in Fig. 13. Here R1 is the resistance of the electrolyte, R2 is the resistance of the chemical reaction, CPE1 (C_1) the imperfect capacitance of the adsorption free surface, R3 the charge transfer resistance and CPE2 (C_2) the imperfect capacitance of the part of surface with adsorbed $CuCl^-_{ads}$. The magnitude of the

parameters calculated with this equivalent circuit is shown in Table 3. The spectra measured at the highest potential, +0.45 V, Fig. 10 showed a clear tail in the phase angle at the lowest frequencies, indicating a transport process, most probably diffusion of CuCl(aq) outwards from the solution. This was taken into account in the equivalent circuit at the high potential by adding another constant phase element, CPE3 in series with R3.

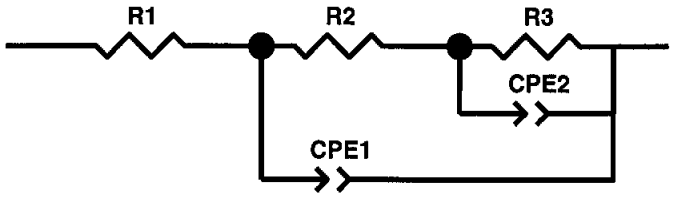

Figure 13. Equivalent circuit for the corrosion reaction scheme proposed by Gabrielli et al. /6/.

Table 3. *Best-fit parameters for the impedance spectra of Cu OFP measured at open circuit Cu OFP in highly saline groundwater at T = 80 °C.*

Test run	Note	R_1 Ω cm^2	R_2 Ω cm^2	C_1 μF cm^{-2}	R_3 Ω cm^2	C_2 μF cm^{-2}	C_3 μF cm^{-2}
1	ocp	0.050	0.19	10900	62.4	53400	
2	ocp	0.045	1.06	37900	96.7	27200	
3	ocp	0.049	0.19	11400	71.7	53500	
4	0.35 V	0.047	0.16	4200	357	29000	
5	0.40 V	0.047	0.15	5700	235	38600	
6	0.45 V	0.044	0.92	22500	22.1	35200	70500

The following equation relates the capacitance C with the distance d of the capacitor surfaces (here ε and ε_0 are the permeability coefficient of the medium and permeability of vacuum, respectively)

$$C = \frac{\varepsilon \cdot \varepsilon_0 \cdot A}{d} \qquad (7)$$

Based on this equation, the capacitance values in Table 3 and using ε = 100 the distance d is less than one atomic layer. This indicates that the processes occur at an interface, which supports the conclusion that the process in question is dissolution from a bare surface.

From corrosion point of view, the process which shows the highest resistance becomes rate limiting. In this case, using the model of Fig. 13 for interpretation of the impedance data the rate limiting process is the charge transfer reaction, having a resistance of the order of 100 Ωcm^2. However, it is also possible that the rate of the process is limited by the cathodic reaction. Because of the very low oxygen content in the solution the diffusion of oxygen to the surface may be the rate-limiting step. To investigate this we calculated from the corrosion rate measured with the corrosion coupons the corresponding polarisation resistance.

Assuming that the anodic process is a one step reaction with Tafelian electron transfer and the cathodic reaction is diffusion limited the following formula applies /9/

$$R_p = \frac{b_a}{2.303 \cdot j_{corr}} \tag{8}$$

Here R_p = polarisation resistance (impedance at the limit f $\rightarrow$ 0 Hz), b_a = anodic Tafel slope and j_{corr} = corrosion current.

The corrosion current can be estimated based on the corrosion rate Δ calculated from the weight loss measurements. This relation is shown by equation

$$j_{corr} = \frac{\Delta \cdot z \cdot \rho \cdot F}{M} \tag{9}$$

Here z is the charge of the ion (in this case +1), F is Faradays constant, $9.6487 \cdot 10^4 Cmol^{-1}$, M is the molar mass of copper, 63.54 $gmol^{-1}$, and ρ the density of copper, 8.94 gcm^{-3}. Assuming that the Tafel slope b_a is 0.1 V /5/ and taking Δ = 0.02 mm/y the corrosion current becomes $j_{corr} = 8.6 \cdot 10^{-7} A \cdot cm^{-2}$ and the polarisation resistance R_p = 50400 Ωcm^{-2}. This value is roughly two orders of magnitude larger than the measured charge transfer resistance R3, see Table 3. This indicates that the corrosion rate is probably not limited by the charge transfer reaction designated by R3 but instead by diffusion of oxygen towards the surface. This process would be seen in the impedance spectra as a Warburg-impedance (phase angle showing a horizontal tail of about 20° to 40°) at very low frequencies, which were not attainable in the present experimental arrangement within a reasonable testing time. This is a general limitation of the EIS technique in a case where a slow reaction in parallel to a faster one determines the overall reaction rate.

Ogundele and Jain /10/ determined the corrosion rate of CuOFP in the Standard Canadian Shield Saline Solution (SCSSS, 0.97 M Cl^- $\cong$ 34400 ppm, atmospheric pressure, nitrogen bubbling) by accelerated electrochemical technique, specifically determination of Tafel slopes within $\pm$ 15 mV from the open circuit potential. From the polarisation resistance measurement they estimated that the corrosion rate at 75 °C at pH_{RT} = 7 is 0.0024 mm/y. In their tests the corrosion rate at 75 °C was almost constant when pH was varied from 4 to 10. The corrosion rate measured in this work was almost

a factor of 10 higher than that found by Ogundele and Jain. This difference may be due to the difference in pressure of the environment (0.1 MPa vs. 14 MPa), the difference in the temperature (75 °C vs. 80 °C) or salinity (0.97 M vs. 1.5 M Cl^-). Increase in any of these three test parameters is expected to increase the measured corrosion rate.

5 CONCLUSIONS

The main conclusions made are:

- Pressure has a clear effect on the voltammetric and EIS behaviour of Cu OFP in highly saline groundwater. Thus, this kind of tests should be performed at the representative pressure of 14 MPa.

- The corrosion potential of Cu OFP in all test runs in the highly saline groundwater was in the range -0.15 $V_{SHE} < E_{corr} < -0.08$ V_{SHE}.

- At the corrosion potential active dissolution (corrosion) of Cu OFP takes place. The corrosion rate was 0.02 mm/y estimated based on the weight loss measurement of coupons exposed to the environment for seven days.

- The mechanism of copper dissolution in highly saline groundwater at 80 °C and 14 MPa is suggested to occur via the reactions

$$Cu + Cl^- \rightarrow CuCl_{ads}^- \qquad \text{chemical reaction}$$

$$CuCl_{ads}^- \rightarrow CuCl(aq) + e^- \qquad \text{electrochemical reaction}$$

  where the reaction intermediate $CuCl^-_{ads}$ is adsorbed onto the surface and is then further oxidised to *CuCl(aq)*.

- The measurement results are in line with the thermodynamic calculations presented in the SKI Report 98:19, concerning the influence of Cl^- content on the dissolution of copper.

6 REFERENCES

/1/ Vuorinen, U. and Snellman, M., Finnish reference waters for solubility, sorption and diffusion studies. Posiva Working Report 98-61. Posiva Oy, December 1998.

/2/ Beverskog, B. and Puigdomenech, I., Pourbaix diagrams for the system copper-chlorine at 5-100 °C. SKI Report 98:19, 1998. Swedish Nuclear Power Inspectorate, Stockholm. 18 p. + app. 16 p.

/3/ Bojinov, M., Fabricius, G., Laitinen, T., Saario, T. and Sundholm, G., Conduction mechanism of the anodic film on chromium in acidic sulphate solutions. Electrochimica Acta. Vol. 44 (1998) No: 2-3, 247 - 261

/4/ Bojinov, M., Fabricius, G., Laitinen, T., Mäkelä, K., Saario, T. and Sundholm, G., Conduction mechanism of the anodic film on Fe-Cr alloys in sulphate solutions. Journal of the Electrochemical Society. Vol. 146 (1999) No: 9, 3238 - 3247.

/5/ Deslouis, C., Tribollet, B., Mengoli, G. and Musiani, M., Electrochemical behaviour of copper in neutral aerated chloride solution. I . Steady-state investigation. Journal of applied electrochemistry, Vol. 18, pp. 374-383, 1988.

/6/ Gabrielli, C., Keddam, M., Minouflet-Laurent, F. and Perrot, H., Simultaneous EQCM and ring-disc measurements in AC regime. Application to copper dissolution. Electrochemical and solid-state letters, Vol. 3, pp. 418-421, 2000.

/7/ King, F. and Kolar, M., Prediction of the lifetimes of copper nuclear waste containers under restrictive mass-transport and evolving redox conditions. Corrosion NACE 1995, paper No. 425, 28 p.

/8/ King, F. and Tang, Y., The anodic dissolution of copper in chloride-sulphate groundwaters. Report No 06819-REP-01200-0058 R00. Ontario Hydro, Nuclear Waste Management Division. Toronto. 35 p. + app. 15 p. August 1998.

/9/ Gabrielli, C., Identification of electrochemical processes by frequency response analysis. Technical Report Nr. 004, 1984. Solartron Ltd, France; Epelboin, I., Gabrielli, C., Keddam, M. and Takenouti, H., Proc. of the ASTM Symposium "Progress in Electrochemical Corrosion Testing", May 1979. Ed. F. Mansfeld and U. Bertocci, pp. 150-166, 1981. ASTM.

/10/ Ogundele, G. and Jain, D., Abiotic corrosion of Finnish OFP copper in standard Canadian Shield saline solution (SCSSS). Report No 06819-REP-01200-0057R00. Ontario Hydro, Nuclear Waste Management Division. Toronto. 32 p. + app. 17 p. June 1998.